



This is a repository copy of *Cerebellum-based Adaptation for Fine Haptic Control over the Space of Uncertain Surfaces*.

White Rose Research Online URL for this paper:  
<http://eprints.whiterose.ac.uk/108455/>

Version: Accepted Version

---

**Proceedings Paper:**

Barron-Gonzalez, H., Porrill, J., Lepora, N.F. et al. (3 more authors) (2013)  
Cerebellum-based Adaptation for Fine Haptic Control over the Space of Uncertain Surfaces. In: World Haptics Conference (WHC), 2013. 2013 World Haptics Conference (WHC), April 14 - 18, 2013, Daejeon, Korea. IEEE , pp. 353-358. ISBN 978-1-4799-0087-9

<https://doi.org/10.1109/WHC.2013.6548434>

---

© 2013 IEEE. Personal use of this material is permitted. Permission from IEEE must be obtained for all other users, including reprinting/ republishing this material for advertising or promotional purposes, creating new collective works for resale or redistribution to servers or lists, or reuse of any copyrighted components of this work in other works.

**Reuse**

Unless indicated otherwise, fulltext items are protected by copyright with all rights reserved. The copyright exception in section 29 of the Copyright, Designs and Patents Act 1988 allows the making of a single copy solely for the purpose of non-commercial research or private study within the limits of fair dealing. The publisher or other rights-holder may allow further reproduction and re-use of this version - refer to the White Rose Research Online record for this item. Where records identify the publisher as the copyright holder, users can verify any specific terms of use on the publisher's website.

**Takedown**

If you consider content in White Rose Research Online to be in breach of UK law, please notify us by emailing [eprints@whiterose.ac.uk](mailto:eprints@whiterose.ac.uk) including the URL of the record and the reason for the withdrawal request.



[eprints@whiterose.ac.uk](mailto:eprints@whiterose.ac.uk)  
<https://eprints.whiterose.ac.uk/>

# Cerebellum-based Adaptation for Fine Haptic Control over the Space of Uncertain Surfaces

Hector Barron-Gonzalez<sup>\*1</sup>, John Porrill<sup>1</sup>, Nathan F. Lepora<sup>1</sup>, Eris Chinellato<sup>2</sup>, Giorgio Metta<sup>3</sup>, and Tony J. Prescott<sup>1</sup>

<sup>1</sup>Sheffield Centre for Robotics, Department of Psychology, University of Sheffield, UK.

<sup>2</sup>Intelligent Systems and Networks Group, Electrical and Electronic Engineering, Imperial College of London, UK.

<sup>3</sup>Department of Robotics, Brain and Cognitive Sciences, Istituto Italiano di Tecnologia, Italy.

## ABSTRACT

This work aims to augment the capacities for haptic perception in the iCub robot to generate a controller for surface exploration. The main task involves moving the hand over an irregular surface with uncertain slope, by concurrently regulating the pressure of the contact. Providing this ability will enable the autonomous extraction of important haptic features, such as texture and shape. We propose a hand controller whose operational space is defined over the surface of contact. The surface is estimated using a robust probabilistic estimator, which is then used for path planning. The motor commands are generated using a feedback controller, taking advantage of the kinematic information available by proprioception. Finally, the effectiveness of this controller is extended using a cerebellar-like adapter that generates reliable pressure tracking over the finger and results in a trajectory with less vulnerability to perturbations. The results of this work are consistent with insights about the role of the cerebellum on haptic perception in humans.

**Keywords:** Haptic perception, robot sensorimotor control, tactile exploration

**Index Terms:** I.2.9 [Artificial intelligence]: Robotics—Kinematics and dynamics/Manipulators

## 1 INTRODUCTION

Robots are required to have high dexterity to interact with surrounding objects, as humans do. Coarse exploration of objects has been widely explored through grasping-based actions, but fine exploration remains an open problem because it requires of accurate movements to sensibly manipulate objects or extract important tactile information. For example, the tactile perception of texture or shape has mainly been achieved with robots making reproducible actions in simple environments [6]. An important task in fine exploration is to place the hand over an unknown surface and slide it while regulating the pressure of the contact. Tactile arrays and soft fingers have been commonly used to execute this exploratory procedure, in order to achieve surface recognition [8] or reconstruction [12]. Specifically, the work in [11] relies on a soft fingertip that allows measuring the contact force from any direction. An hybrid velocity-force controller [15] is used to regulate the finger compliance with respect to the shape of the explored object. Using a similar type of sensor, Karayiannidis and Doulgeri [5] use a force-position controller to estimate the slope of the surface and regulate the intensity of the contact. The dynamic parameters of a three-link manipulator are adapted using feedback from force sensors. On the other hand, the work in [1] addresses the problem of explor-

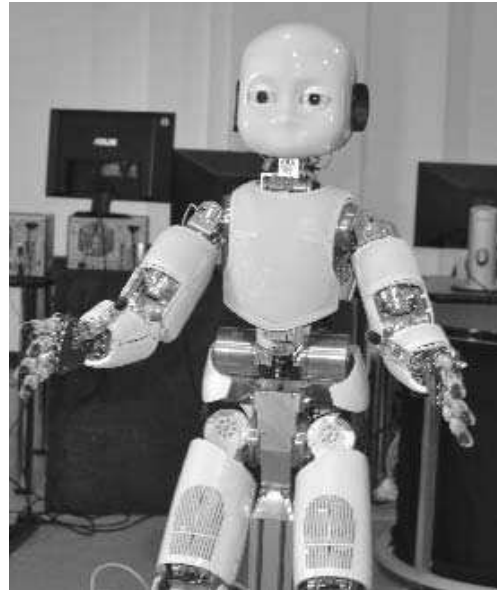


Figure 1: The iCub robot

ing the surface when the contact is also compliant. In this case, the controller is based on a neural network that learns the dynamic characteristics of the surface. In all these cases, information about dynamics of the manipulator and force sensor are available.

We are interested in implementing such dexterity in the child-like iCub android (see Fig. 1). Each upper limb is controlled by 16 degrees of freedom (DOF): seven for the arm and nine for the hand [13]. An encoder is paired with each joint to capture proprioceptive information. The android hand has soft fingertips with rubber-covered sensors oriented towards the hand palm. However, the haptic interaction with the environment requires a careful plan for avoiding any physical damage to the robot. Its fingers are operated via a tendon-based actuation system that produces nonlinearities projected as springiness effects. The problem has a further challenge that the contact between the hand and surface has to maintain constant pressure during the exploration, for which there is no available information for the torque at the fingers, which is an important difference with respect to related work.

We require a hand controller whose operational space is defined over a surface of contact with unknown height and slope. Due the accuracy and sampling rate of the encoders, tests upon the real robot have showed us that finger deflection might be more reliable than the tactile sensors for detecting contact. Hence, the proposed controller aims to regulate the contact pressure, using the measurements of the finger joints. In order to achieve the optimal

\*e-mail: hector.barron@shef.ac.uk



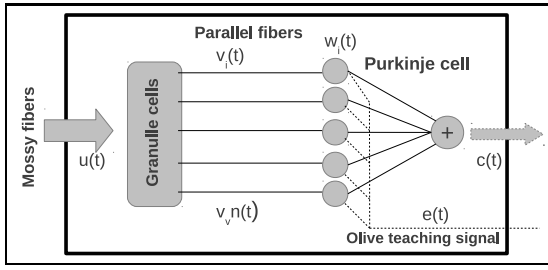


Figure 3: Adaptive filter model of cerebellar microcircuit. The mossy fiber input  $u(t)$  are encoded by granule cells, whose axons form parallel fibers  $v_i(t)$  with synapse on Purkinje cells.

### 3.2 Cerebellar model

The Purkinje cells of the cerebellar cortex receive excitatory inputs from parallel fibers, which are granule cell axons [9]. These granule cells are excited by mossy fibers with afferent connections from the spinal cord. Each Purkinje cell receives further excitatory synapses from a single climbing fiber that originates from inferior olivary neurons. This connection is important because it can act as a teaching signal to regulate the firing of Purkinje cells in response to their parallel fiber inputs. This cerebellar microcircuit has been conceived of as an adaptive filter, and is related to the *Marr-Albus* model of cerebellar function [4, 7]. This model is illustrated in Fig. 3. The input signal  $u(t)$ , comprising motor and sensory signals, is firstly processed by bank of filters  $G_i$ , which provide a simplified model of the granule cells [4]. These filters transform the input signal into an expanded array of parallel fiber signal  $v_i(t)$ . Here the filters  $G_i$  are based on a set of radial basis functions (*RBF*) that provides a set of encoded delayed input data for the adaptive layer of the filter.

The output of the Purkinje cells is modelled as a weighted sum of these parallel fiber signals, with the weights corresponding to synaptic efficacies. The climbing fiber input is then interpreted as a teaching signal  $e(t)$  that originates from the inferior olive, which adapts the synaptic weights. The temporal correlation between the parallel fiber and teaching signal is used to modify each weight  $w_i(t)$  through the following covariance learning rule

$$\Delta w_i(t) = -\beta(v_i(t) - \bar{v}_i)(e(t) - \bar{e}) \quad (6)$$

where  $\beta$  is the learning rate, and  $\bar{v}_i$  and  $\bar{e}$  are mean values of  $v_i(t)$  and  $e(t)$ , respectively. Finally, the olivary neuron utilizes perceptual information to infer an error measurement that is used to regulate the motor coordination. Perceptual information could be generated from diverse sources (e.g. from visual or tactile sensors).

## 4 CONTROLLER

The general scheme to control the surface exploration is illustrated in Fig. 4. First, the orientation of the surface is estimated, using the real displacement of the hand. Second, the trajectory and pose of the end effector are defined in the operational space. Then, the motor commands are transformed into actuator primitives within the joint space. Finally, a cerebellar-like structure is integrated to generate motor corrections. The rest of the section describes each part of this controller.

### 4.1 Observer of the surface orientation

The trajectory and pose of the hand has to be determined by the shape of the surface. The main strategy is to move the end effector perpendicularly to the surface normal vector. Because the surface state is uncertain, the surface axes have to be estimated while exploring. This paper proposes a probabilistic observer that holds the

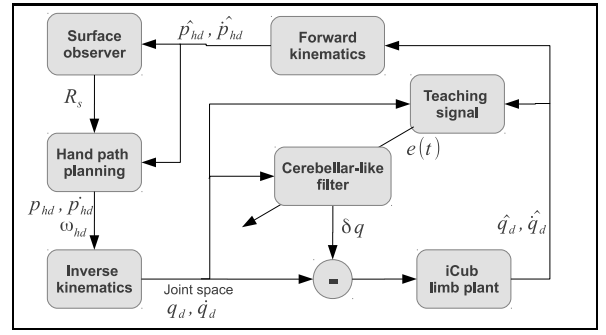


Figure 4: Controller for surface exploration. The orientation of the surface  $R_s$  is estimated utilizing the measured velocity of the hand. Meanwhile, the distance between the surface and the hand is regulated by the cerebellar-like structure, utilizing the finger deflection.

tracking onto the slope of the surface and gradually updates its estimates.

While displacing the hand over the surface, it is convenient to align the axis  $o_s$  with respect to the unitary directional vector of the hand movement, tangential to the surface. Note that the desired hand displacement and velocity have been already defined with this assumption in Section 2. In this case, the axis  $a_s$  consists on the other tangential vector over the surface, perpendicular to the hand movement, which should be kept constant whilst the rest of the axes are being estimated. The estimation of the normal vector  $\bar{n}_{s,t}$  at time  $t$ , is directly computed by the cross product

$$\bar{n}_{s,t} = \bar{a}_{s,t} \times \bar{o}_{s,t} \quad (7)$$

where  $\bar{a}_{s,t}$  is the estimated axis  $a_s$ . The coordinates of the estimated axis  $\bar{o}_{s,t} = [o_{x,t}, o_{y,t}, o_{z,t}]$  are correlated by the normalization of this directional vector. Hence, the observer can only focus on estimating the vertical coordinate  $o_{z,t}$  of the surface using the instant displacement of the hand.

From (3), the vertical coordinate  $z_h$  of the desired hand velocity  $\dot{p}_{hd}$  is computed by

$$z_h = \bar{R}_{[s,3]} \dot{p}_{sh} \quad (8)$$

where  $\bar{R}_{[s,3]}$  is the third row of the current rotation matrix  $\bar{R}_s$ . Let  $J_{[3]}(\hat{q})$  be defined as the third row of the kinematic Jacobian, parameterized by the current joints measurement  $\hat{q}$ . Thus, the measurement of the vertical hand displacement can be computed by

$$\hat{z}_h = J_3(\hat{q})\hat{q} \quad (9)$$

In addition, the measurement noise from the joints can be modeled by its covariance  $\Sigma_q$ , which can be transformed into operational units through uncertainty propagation by

$$\Sigma_z = J_3(\hat{q})\Sigma_q J_3^T(\hat{q}) \quad (10)$$

Then, the innovation  $v$  and its covariance  $S$  are computed by

$$v = z_h - \hat{z}_h \quad (11)$$

$$S = \dot{p}_{sh}^T \Sigma_O \dot{p}_{sh} + \Sigma_z \quad (12)$$

where  $\Sigma_O$  represents the expected variability in the elevation of the explored surface. Finally, the vertical coordinate  $o_{z,t}$  of the surface frame axis  $o_s$  is estimated by the following update law

$$o_{z,t} = o_{z,t-1} + Kv \quad (13)$$

where  $K$  is the appropriate Kalman gain computed by

$$K = \hat{p}_{sh}^T \Sigma_O \hat{p}_{sh} S^{-1} \quad (14)$$

The estimates  $\bar{n}_{s,t}$  and  $\bar{o}_{s,t}$  are used to update  $R_s$  in each instant of the time, describing the surface orientation at the point that is being currently touched.

## 4.2 Generation of motor commands

With the estimation of the surface orientation, the desired trajectory and pose of the hand are updated by (1)-(4). Then, the generation of motor commands requires the computation of a reference velocity vector in the operational space.

First, let  $e_p$  and  $e_o$  be defined as the position and orientation error of the end effector, computed by

$$e_p = p_{hd} - \hat{p}_h \quad (15)$$

$$e_o = \frac{1}{2} (\hat{n}_h \times \bar{n}_h + \hat{o}_h \times \bar{o}_h + \hat{a}_h \times \bar{a}_h) \quad (16)$$

where the measured hand position  $\hat{p}_h$  and observed hand orientation matrix  $\hat{R}_h = [\hat{n}_h, \hat{o}_h, \hat{a}_h]$  could be computed by direct kinematics using the current joint positions. Differentiating (15) and (16), the respective velocity error is

$$\dot{e}_p = \dot{p}_{hd} - \dot{\hat{p}}_h \quad (17)$$

$$\dot{e}_o = L^T \omega_{hd} - L \dot{\omega} \quad (18)$$

$$L = -\frac{1}{2} (S(\bar{n}_h)S(\hat{n}_h) + S(\bar{o}_h)S(\hat{o}_h) + S(\bar{a}_h)S(\hat{a}_h)) \quad (19)$$

and  $S(\cdot)$  is the skew-symmetric operator [15].

Then, the measured error can be used as feedback in a PID controller upon the operational space, computing the velocity-based motor commands [5] by

$$\begin{bmatrix} \dot{p}_c \\ \omega_c \end{bmatrix} = \begin{bmatrix} \dot{p}_{hd} - \alpha Q e_p - \beta \frac{\bar{n}_s}{\|\bar{n}_s\|} \Delta_h - \Gamma I h \\ L^T \omega_{hd} - \gamma e_o \end{bmatrix} \quad (20)$$

where  $\alpha$ ,  $\beta$ ,  $\Gamma$  and  $\gamma$  are control parameters, the matrix  $Q$  projects the error position over the tangential plane of the surface and the vector  $\bar{n}_s/\|\bar{n}_s\|$  is the component of a force-based differential during the contact over the normal vector of the surface. The term  $Ih$  is the accumulative term of the force-based differential  $\Delta_h$ .

The joint-level commands are based on the built-in velocity-based control implemented on the iCub. Using inverse kinematics, these commands are generated directly from the reference velocity in (20), by

$$\dot{q} = J^\dagger L_0^{-1} \begin{bmatrix} \dot{p}_c \\ \omega_c \end{bmatrix} \quad (21)$$

$$L_0 = \begin{bmatrix} 1 & 0 \\ 0 & L \end{bmatrix} \quad (22)$$

and  $J^\dagger$  is the Moore-Penrose pseudoinverse. Here the robot arm is better considered as a redundant manipulator because of its seven degrees of freedom.

With reference to the normal component in (20), the contact force is kinetically measured by the deflection over the fingers caused by the interaction with the surface. Thus, the differential  $\Delta_h$  could be computed as the Euclidean distance of the current finger joint position  $\hat{q}_f$  and the desired finger joint state  $q_{fd}$ . It is important to notice that this relation is, in fact, dependent on the dynamic parameters of the finger by (5), which are usually unknown. In order to compensate this uncertainty, the joint-based control commands are corrected by a cerebellar-like structure, as defined in

Section 3 and illustrated in Fig. 4. This component serves as an adaptive filter that attempts to reduce a teaching error signal.

The proposed architecture of the cerebellar-like structure consists of several different layers. The input layer, representing the mossy fibers and granule cells, is divided in  $n_i = 14$  groups of  $n_c$  cells. Seven groups carry information about the desired joint position and the other seven code the desired joint velocity, using one group per joint. The receptive fields of the granule cells are simplified to a set of overlapping Gaussian functions with mean  $\mu_i$  and standard deviation  $\sigma_i$ . The Purkinje layer is composed of seven cells that output synaptically weighted combinations of the outputs of the granule cells. The output of the Purkinje cells provides the direct correction to each joint. The synaptic weights are updated by a teaching signal computed as the kinematic error perceived at each joint  $i$  by

$$e_i = K_p (\bar{q}_i - \hat{q}_r) + K_v (\dot{\bar{q}}_i - \dot{\hat{q}}_r) + K_h \Delta_h \quad (23)$$

where  $K_p$ ,  $K_v$  and  $K_h$  are constant gains. This teaching error does not only carry information about the desired hand pose but also about the desired finger deflection.

## 5 EXPERIMENTS

The experiments reported in this paper are aimed at demonstrating the efficacy of the controller. The tests were carried out in the iCub simulator [18] to evaluate the accuracy of the estimates. The left arm of the robot was used to execute the exploration, which has seven degrees of freedom. The hand was set in a pointing position, allowing use of the index finger as pressure sensor. The simulator allows controlling the finger joints of the hand using position and velocity commands. Tactile sensors are also available as discrete indicators of contact, located on the hand palm and fingertips. Nevertheless, we did not use these sensors here because we focused to exploit the information provided by the finger deflection during contact. Further work with real robot might involve integration of tactile measurements for contact detection. Because the stiffness of the finger is not part of the in-built simulation, it was implemented using the dynamic model in (5), considering a three-link structure with revolute joints such as described in [13]. Each link has mass  $m_i = 0.5$  grams, length  $l_i = 0.03$  m and inertial computed by  $I_{i,i} = m_i * l_i^2 / 3$ . The friction coefficient over the joints was not considered in these tests. The flexibility of each joint was simulated with the function  $P(q) = -k_{\text{suff}}(\hat{q} - q_0) - k_{\text{damp}}\dot{q}$  where  $q_0 = [15^\circ, 20^\circ]$  is the set of initial joint positions,  $k_{\text{suff}} = 0.001$  and  $k_{\text{damp}} = 0.0001$  are the stiffness and the damping factors, respectively. The surface stiffness  $k_s = 8.0$  was utilized to compute the external force of contact.

The controller was used to compute the values in 7 out of 16 degrees of freedom in the arm (three for shoulder, one for elbow and three more for wrist). The rest of the joints were held fixed. Though the high dimensionality of the motor command, only the dynamics of two finger joints (index finger) was to be compensated by the adaptive filter. The contribution of each arm joint, to generate a regulated contact pressure, was defined by the kinematic Jacobian. This was used directly to compute the desired joint positions and velocities in (23).

Two different scenarios are described in rest of this section. The first scenario involves exploration over a sloped planar surface with time-varying pressure. The second scenario considers moving the hand over an irregular surface. Additionally, the convergence of the olivary error was empirically observed with simplified experiments to define the values of the cerebellar parameters. For instance, holding a desired hand velocity of 0.0 m/s, the control with different parameters was evaluated. Meanwhile a fixed surface was used to establish the value of the cerebellar parameters in scenario 1, a mobile surface was utilized to define the parameters in scenario 2. Varying the number of granule cells did not produce a critical

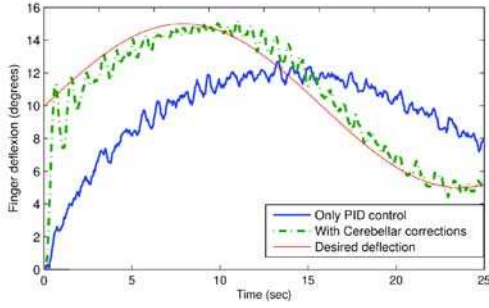


Figure 5: Pressure tracking by the finger. The original controller presents a lag when tries to follow the requested finger deflection (solid blue-line). The cerebellar adapter reduces this delay (dashed green line).

impact over the reduction of the olivary error. However, the length of the baseline memory was an important factor because a reduced time lapse could degenerate the olivary signal into a periodical behavior. When the cerebellar structure generated an adequate result, the whole scenarios were evaluated.

### 5.1 Scenario 1

The iCub reference frame is located at the middle of its waist, with the  $X$ -axis aligned backwards and  $Z$ -axis aligned upwards. The robot initialization consisted of having the fingertip pointing downwards at the point  $p_0 = [-0.3m, -0.18m, 0.20m]$ . The initial hand orientation was  $o_0 = [-0.1, 0, 0.9, 3.14 rad]$ , defined in axis-angle notation. The planar surface was situated to  $0.03m$  from the fingertip and had a slope of  $15$  degrees. The desired velocity of the hand over the surface was set to  $\dot{p}_{sh} = 0.015 m/s$ , such that the hand was displaced towards the right of the iCub. The time-varying pressure exerted by the contact was defined by the normal of the finger joint deflection, defined by  $q_{fd} = 10 \sin(t)$ . The gains of the controller were  $\alpha = 0.8$ ,  $\beta = 0.006$ ,  $\Gamma = 0.002$  and  $\gamma = 0.5$ . The gains  $\beta$  and  $\Gamma$  would be the proportional and integrative factors in a PID controller taking the finger deflection error as input. The cerebellar structure contains  $n_c = 50$  granule cells in each group. The means  $\mu_i$  of their receptive fields were located along the range of possible input values with standard deviation  $\sigma_i = 1.5$ . The baseline  $\bar{p}_i$  and  $\bar{e}$  in (6) were computed with a memory of  $0.5$  sec. The learning rate was defined by  $\beta = 0.007$ . The olivary error was computed using the factors  $K_p = 0.35$ ,  $K_i = 0.20$  and  $K_f = 0.45$ .

The controller was evaluated with and without cerebellar corrections. The performance during exploration was acceptable in both cases, because the contact maintenance was fully achieved. However, there were significant differences in robustness. Fig. 5 illustrates the tracking of the requested finger deflection after 50 Monte Carlo runs. The controller without cerebellar correction displayed a significant lag during the tests. This lag is caused by the processing time and inaccurate gains for the control. The PID control runs were used for training of the cerebellar-like structure. The cerebellar corrections provided the controller with the information required to reduce the lag and achieve reliable tracking over the requested finger deflection. The distance between the surface and the corrected hand showed more variability than the PID-controlled hand (see Fig. 6). Nevertheless, this movement is mainly caused by the regulation of the pressure according to desired finger deflection. The capability of dynamically regulating the pressure will allow the robot to perceive different haptic features. Fig. 7 illustrates the angular difference between the orientation of the hand and the surface normal at the point of contact. Although both cases provided an adequate capability for adjusting the pose of the hand with respect to

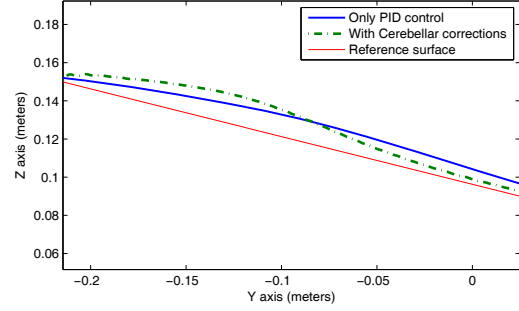


Figure 6: Hand position over surface during exploration. The correction of the finger deflection is projected as changes of distance between the surface and the position of the palm of the hand.

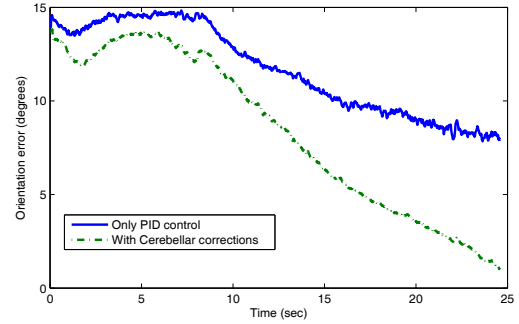


Figure 7: Hand orientation error. The angular error is shown between the hand and the surface normal at the contact point.

the surface, the cerebellar structure allowed alignment of the hand with superior performance. We note that, similarly, the human hand also adjusts its alignment to extract tactile information based on the hand position.

### 5.2 Scenario 2

In the second set of tests, the surface to be explored is defined by a fourth degree polynomial curve, defined by the function  $z = 200.0y^4 - 100.0y^3 - 19.0y^2 + 0.2$  where  $y$  is the horizontal coordinate of the surface in the robot frame of reference. The gains of the controller were  $\alpha = 0.8$ ,  $\beta = 0.0001$ ,  $\Gamma = 0.0035$  and  $\gamma = 0.5$ . The desired velocity of the hand over the surface was set to  $\dot{p}_{sh} = 0.01 m/s$ . The cerebellar model contained  $n_c = 75$  gran-

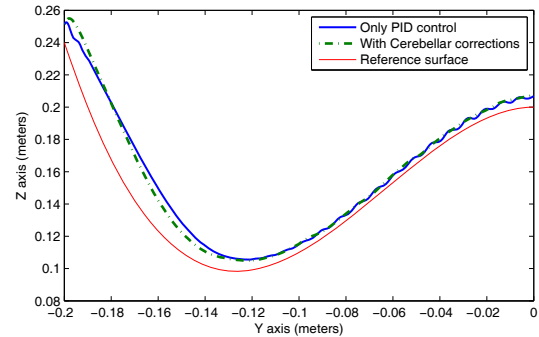


Figure 8: Hand position in exploration over polynomial surface.

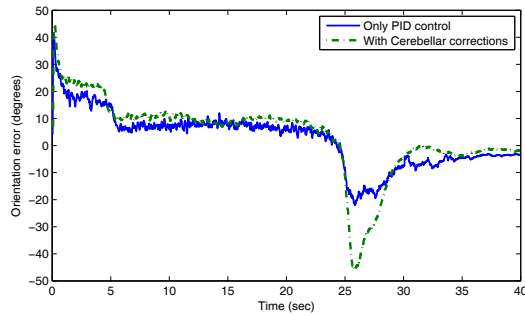


Figure 9: Hand orientation. The angular error is shown between the hand and the polynomial surface normal at the contact point.

ule cells in each group. The receptive fields had standard deviation  $\sigma_i = 0.5$ . The baselines  $\bar{p}_i$  and  $\bar{e}$  were computed with a memory of 0.75sec and the learning rate was  $\beta = 0.01$ . The olivary error was computed using the factors from the first scenario. The requested finger deflection was kept constant at 10 degrees. The hand position during exploration and the angular error of the hand pose are illustrated in Figs 8 and 9, after 50 Monte Carlo runs. When the hand is going downwards, both cases are able to hold close contact with the surface. There is a slight initial perturbation in the corrected trajectory, possibly caused by the cerebellar adaptation. In the second part of the trajectory, the hand without the cerebellar correction showed dramatic oscillating movements, caused mainly by dynamical effects of the finger and the estimation of the varying slope. The cerebellar-controlled hand reduced such effects, generating a smoother movement.

The angular error between the surface normal and the hand orientation is also similar between two cases. However, the cerebellar adapted trajectory suffered a slight delay to align the hand with the surface when the hand started going upwards. This could be caused by conditioning the filter during the first part of the path. Finally, the hand had a fast correction of its pose before the end of movement.

## 6 CONCLUSIONS

The experiments reported in this paper illustrated the performance of surface-following controller for haptic exploration. First, we achieved appropriate movements of the hand that adapted its pose with respect to the surface. And second, we demonstrated how the cerebellar-like adapter is used to achieve greater robustness during exploration, by regulating the contact to generate a trajectory with less perturbations.

This paper also illustrates how different components can be integrated to reliably solve a motor control task, providing insights into how haptic exploration is performed in humans. The high-level component of the controller is determined by the estimation of the surface orientation, whose functionality could correspond to the process of spatial perception in parietal lobe. This hypothesis leads to the proposal that the cerebellum might not be the main generator of movement, but instead provides low-level motor commands to regulate the force and velocity of the movement during tactile exploration.

Further research will involve to analyze the performance of the controller upon the iCub, extending the perceptual capacities of the real android for identifying haptic features. Finally, by implementing neural-inspired mechanisms for control in humanoid robots, we gain insight into the mechanisms by which humans perceive and interact with their surroundings.

## ACKNOWLEDGEMENTS

The research leading to these results has received funding from the European Union Seventh Framework Programme FP7/2007-2013, under grant agreement No [270490]- [EFAA]

## REFERENCES

- [1] C. P. Bechlioulis, Z. Doulgeri, and G. A. Rovithakis. Neuro-adaptive force/position control with prescribed performance and guaranteed contact maintenance. *Trans. Neur. Netw.*, 21(12):1857–1868, 2010.
- [2] N. H. Bhanpuri, A. M. Okamura, and A. J. Bastian. Active force perception depends on cerebellar function. *Journal of Neuropsychology*, 107:1612–1620, 2012.
- [3] M. Chalon, W. Friedl, J. Reinecke, T. Wimboeck, and A. Albu-Schaeffer. Impedance control of a non-linearly coupled tendon driven thumb. In *Intelligent Robots and Systems (IROS), 2011 IEEE/RSJ International Conference on*, pages 4215–4221, 2011.
- [4] P. Dean, J. Porrill, C. F. Ekerot, and H. Jorntell. The cerebellar microcircuit as an adaptive filter: experimental and computational evidence. *Nature Reviews Neuroscience*, 11:30–43, 2010.
- [5] Y. Karayiannidis and Z. Doulgeri. Adaptive control for frictional robot contact tasks on uncertain surface slopes. In *Proceedings of the 16th Mediterranean Conference on Control and Automation*, pages 932–937, 2008.
- [6] N. Lepora, C. Fox, M. Evans, M. Diamond, K. Gurney, and T. Prescott. Optimal decision-making in mammals: insights from a robot study of rodent texture discrimination. *Journal of The Royal Society Interface*, 9(72):1517–1528, 2012.
- [7] N. F. Lepora, J. Porrill, C. H. Yeo, and P. Dean. Sensory prediction or motor control? application of marr-albus type models of cerebellar function to classical conditioning. *Frontiers in Computational Neuroscience*, 4:1–12, 2010.
- [8] H. Liu, X. Song, J. Bimbo, L. Seneviratne, and K. Althoefer. Surface material recognition through haptic exploration using an intelligent contact sensing finger. In *Intelligent Robots and Systems (IROS), 2012 IEEE/RSJ International Conference on*, pages 52–57, 2012.
- [9] N. R. Luque, J. A. Garrido, and R. R. Carrillo. Cerebellarlike corrective model inference engine for manipulation tasks. *IEEE Transactions on Systems, Man and Cybernetics - Part B: Cybernetics*, 41(5):1299–1311, 2011.
- [10] J. F. Medina. The multiple roles of purkinje cells in sensori-motor calibration to predict, teach and command. *Current opinion in Neurobiology*, 21:616 – 622, 2011.
- [11] A. M. Okamura and M. R. Cutkosky. Haptic exploration of fine surface features. In *Robotics and Automation (ICRA), 1999 IEEE/RSJ International Conference on*, pages 2930–2936, 1999.
- [12] Z. Pezzementi, C. Reyda, and G. Hager. Object mapping, recognition, and localization from tactile geometry. In *Robotics and Automation (ICRA), 2011 IEEE/RSJ International Conference on*, pages 5942–5948, 2011.
- [13] A. Schmitz, U. Pattacini, F. Nori, G. Metta, and G. Sandini. Design, realization and sensorization of a dextrous hand: the icub design choices. In *10th IEEE-RAS International Conference on Humanoid Robots*, pages 186–191, 2010.
- [14] N. Schweighofer, M. A. Arbib, and M. Kawato. Role of the cerebellum in reaching movements in humans. distributed inverse dynamics control. *European journal of Neuroscience*, 10:86 – 94, 1998.
- [15] L. Sciacivco and B. Siciliano. *Modelling and Control of Robots Manipulators*. Springer, 2005.
- [16] D. J. Serrien and M. Wiesendanger. Role of the cerebellum in tuning anticipatory and reactive grip force responses. *Journal of Cognitive Neuroscience*, 11(6):672–681, 1999.
- [17] R. M. Spencer, R. B. Ivry, and H. N. Zelaznik. Role of the cerebellum in movements: control of timing or movement transitions? *Experimental brain research. Experimentelle Hirnforschung. Expérimentation cérébrale*, 161(3):383–396, 2005.
- [18] V. Tikhonoff, A. Cangelosi, P. Fitzpatrick, G. Metta, L. Natale, and F. Nori. An open-source simulator for cognitive robotics research: The prototype of the icub humanoid robot simulator. In *Proc. IEEE Workshop Perform. Metrics Intell. Syst.*, 2008.